

See discussions, stats, and author profiles for this publication at: <https://www.researchgate.net/publication/12493564>

Three-Dimensional Anatomic Characterization of the Canine Laryngeal Abductor and Adductor Musculature

Article in *The Annals of otology, rhinology, and laryngology* · June 2000

DOI: 10.1177/000348940010900512 · Source: PubMed

CITATIONS

20

READS

123

4 authors, including:



Roger W Chan

102 PUBLICATIONS 3,461 CITATIONS

[SEE PROFILE](#)



Ingo R Titze

University of Utah

424 PUBLICATIONS 21,266 CITATIONS

[SEE PROFILE](#)

Some of the authors of this publication are also working on these related projects:



An Optimizer-Simulator for Phonosurgery [View project](#)



singing voice [View project](#)

THREE-DIMENSIONAL ANATOMIC CHARACTERIZATION OF THE CANINE LARYNGEAL ABDUCTOR AND ADDUCTOR MUSCULATURE

COREY W. MINECK, MD
MEMPHIS, TENNESSEE
ROGER CHAN, PHD
IOWA CITY, IOWA

NIRO TAYAMA, MD
TOKYO, JAPAN
INGO R. TITZE, PHD
IOWA CITY, IOWA

The biomechanics of vocal fold abduction and adduction during phonation, respiration, and airway protection are not completely understood. Specifically, the rotational and translational forces on the arytenoid cartilages that result from intrinsic laryngeal muscle contraction have not been fully described. Anatomic data on the lines of action and moment arms for the intrinsic laryngeal muscles are also lacking. This study was conducted to quantify the 3-dimensional orientations and the relative cross-sectional areas of the intrinsic abductor and adductor musculature of the canine larynx. Eight canine larynges were used to evaluate the 3 muscles primarily responsible for vocal fold abduction and adduction: the posterior cricoarytenoid, the lateral cricoarytenoid, and the interarytenoid muscles. Each muscle was exposed and divided into discrete fiber bundles whose coordinate positions were digitized in 3-dimensional space. The mass, length, relative cross-sectional area, and angle of orientation for each muscle bundle were obtained to allow for the calculations of average lines of action and moment arms for each muscle. This mapping of the canine laryngeal abductor and adductor musculature provides important anatomic data for use in laryngeal biomechanical modeling. These data may also be useful in surgical procedures such as arytenoid adduction.

KEY WORDS — abduction, adduction, arytenoid cartilage, laryngeal anatomy, laryngeal muscle, vocal fold.

INTRODUCTION

The physiology and biomechanics of vocal fold abduction and adduction during phonation, respiration, and airway protection (eg, in swallowing) are beginning to be understood on a quantitative level. Traditionally, it has been assumed that each laryngeal muscle functions as a unit, with a single direction of action. However, recent research has demonstrated that at least some of the intrinsic laryngeal muscles are composed of different compartments that may function independently. For example, Sanders et al¹⁻⁴ showed that the posterior cricoarytenoid (PCA) muscle has 2 or 3 separate bellies that may each function as an independent unit during different types of abduction. Sanders et al^{3,4} also showed that the innervation of the human PCA muscle stems from 2 separate nerve branches to supply 2 different compartments, further lending support to independent function. Therefore, it was the purpose of this study to characterize the 3-dimensional (3-D) orientations and relative cross-sectional areas of the laryngeal abductor and adductor muscles for the purpose of biomechanical modeling. The canine larynx was chosen because the active contractile properties of some canine

laryngeal muscles had previously been measured.⁵⁻⁷ Because it is practically difficult to measure the active properties of viable human laryngeal muscles (the tissue must be removed before death), an animal model is desirable, and dogs offer a model similar to the human larynx in laryngeal muscle morphology, anatomy, and possibly function.

The motion of the arytenoid cartilage on the cricoarytenoid joint (CAJ) is complex and has been examined extensively.⁸⁻¹⁴ Classically, arytenoid motion on the CAJ has been described as a rotation around a “vertical” axis.¹⁵ However, many anatomic and vocal fold kinematic studies have suggested that the 2 major arytenoid motions are 1) rocking around the longitudinal axis of the CAJ facet in a somewhat anterior-posterior direction and 2) sliding along this axis in a somewhat medial-lateral direction.^{8,10,11,13,14} Selbie et al¹⁴ showed that the rocking axis could be congruent with the classic “vertical” axis, such that the rocking motion is often perceived as a rotation under the perspective of an endoscope. Current beliefs suggest that the arytenoid motion is critically determined by several major factors, including the geometry of the CAJ facets, the anatomy of the fibro-

From the National Center for Voice and Speech, Department of Speech Pathology and Audiology, University of Iowa, Iowa City, Iowa (all authors), and the Department of Otolaryngology, University of Tokyo, Tokyo, Japan (Tayama). Dr Mineck is currently in the Department of Otolaryngology–Head and Neck Surgery, University of Tennessee, Memphis, Tennessee. This work was supported by grant P60 DC00976 from the National Institutes of Health/National Institute on Deafness and Other Communication Disorders. This study was performed in accordance with the PHS Policy on Humane Care and Use of Laboratory Animals, the NIH *Guide for the Care and Use of Laboratory Animals*, and the Animal Welfare Act (7 U.S.C. et seq.); the animal use protocol was approved by the Institutional Animal Care and Use Committee (IACUC) of the University of Iowa.

CORRESPONDENCE — Roger Chan, PhD, National Center for Voice and Speech, Dept of Speech Pathology and Audiology, 330 WJSHC, University of Iowa, Iowa City, IA 52242.

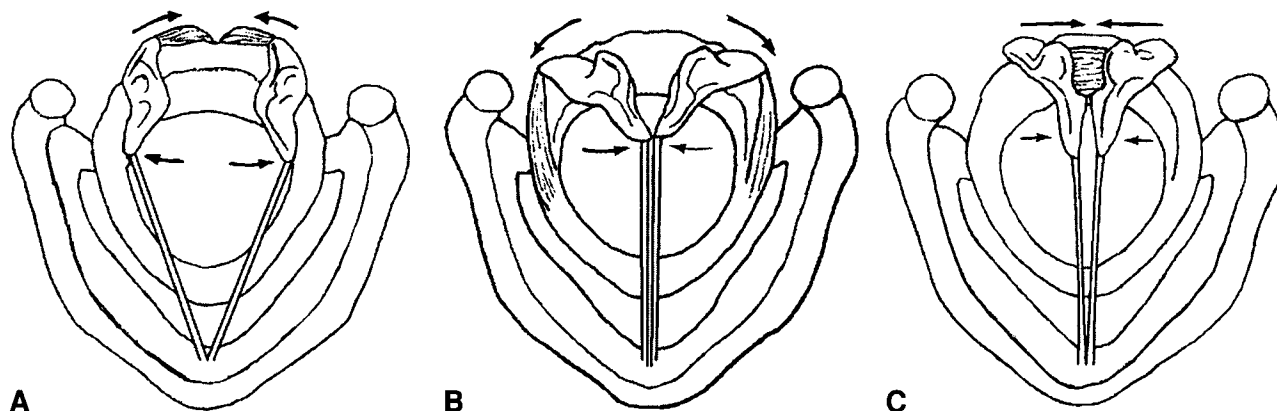


Fig 1. Classic descriptions of arytenoid motion and vocal fold abduction and adduction associated with contraction of A) posterior cricoarytenoid (PCA) muscle, B) lateral cricoarytenoid (LCA) muscle, and C) interarytenoid (IA) muscle. (Copyright 1989. Novartis. Reprinted with permission from the *Atlas of Human Anatomy*, illustrated by Frank H. Netter, MD. All rights reserved.)

elastic connective tissues in the synovial joint, and the actions of the laryngeal abductor and adductor muscles.¹⁶

The laryngeal abductor and adductor muscles are believed to have rapid contraction rates, especially the lateral cricoarytenoid (LCA) muscle.¹⁷ The isotonic twitch contraction time of the canine LCA muscle has been estimated to be on the order of 10 ms, whereas for the PCA muscle, it was around 30 ms.¹⁷ With such rapid contraction times, these muscles play a primary role in the rapid opening of the glottis during inspiration and in rapid closure of the glottis for protection against foreign body inhalation (eg, during swallowing).

The PCA muscle originates at the posterior surface of the lamina of the cricoid cartilage and converges on the laterally directed muscular process of the arytenoid cartilage. This muscle has been described as having 3 parts in dogs and either 2 or 3 parts in humans. For the canine PCA muscle, a horizontal belly, a vertical belly, and an oblique belly have been described by Sanders et al.^{1,2} For the human PCA muscle, Bryant et al¹⁸ described a medial and a lateral belly, but Sanders et al⁴ divided this muscle again into horizontal, vertical, and oblique portions. The PCA muscle rocks the arytenoid posteriorly so that the vocal process swings laterally, superiorly, and posteriorly, abducting the vocal fold (Fig 1A).

The LCA muscle originates on the superior border of the anterior arch of the cricoid cartilage and courses posteriorly to the muscular process of the arytenoid cartilage. The LCA muscle is believed to adduct the vocal fold by rocking the arytenoid cartilage anteriorly such that the vocal process moves medially, inferiorly, and anteriorly¹⁹ (Fig 1B).

The interarytenoid (IA) muscle is composed of a

transverse portion and an oblique portion. The oblique portion originates on the superior aspect of the arytenoid cartilage, crosses the midline, and inserts into the muscular process of the contralateral arytenoid cartilage. The transverse portion connects the lateral borders of the 2 arytenoid cartilages together. Thus, during IA contraction, the arytenoid cartilages are drawn together, adducting the vocal folds (Fig 1C).

This study was conducted to characterize the 3-D orientations and the cross-sectional areas of the intrinsic abductor and adductor musculature of the canine larynx. Data acquired through this study should be useful in establishing a database for 3-D biomechanical modeling of vocal fold posturing. Specifically, they should allow for calculation of the lines of action and moment arms for the intrinsic laryngeal muscles during vocal fold abduction and adduction.

METHODS

Larynges from 4 female and 4 male dogs were excised postmortem after the dogs underwent cardiovascular experimentation in accordance with the Institutional Animal Care and Use Committee of the University of Iowa. No dogs had evidence of trauma or head and neck disease (Table 1). After harvest, the larynges were either slowly or quickly frozen (with

TABLE 1. SUBJECT INFORMATION

Dog	Sex	Weight (kg)
1	F	20
2	M	25
3	M	27
4	F	26
5	M	20
6	F	22
7	M	20
8	F	20

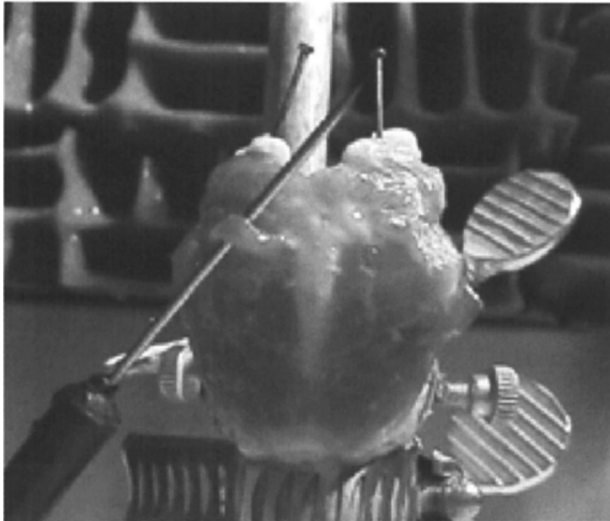


Fig 2. Posterior view of mounted canine larynx shows dissection (isolation) of muscle bundle of left PCA muscle.

liquid nitrogen) and were stored at -20°C . Before dissection, each larynx was thawed overnight in a 4°C refrigerator. Immediately before dissection, larynges were further thawed in physiological saline solution (0.9%).

Each canine larynx was first dissected by means of a blunt instrument technique to expose the PCA, LCA, and IA muscles. Any excess fat or fascial tissue was removed in preparation for mounting and muscle bundle dissection.

The larynx was mounted on a laboratory bench by securing the trachea over a piece of polyvinylchloride tubing with an O-clamp around the first and second tracheal rings. Pincer clamps were used to secure the cricoid cartilage in the anatomic position. The arytenoid cartilages were firmly fixed in the cadaveric position with straight pins such that any rotation or translation of the arytenoid cartilages was eliminated. The larynx was then positioned such that the posterior ridge of the cricoid lamina (the cricoid prominence) between the PCA muscles was vertical (Fig 2).

Once the larynx was mounted, 3-D spatial coordinates for the cricoid cartilage, the arytenoid cartilages, and the laryngeal abductors and adductors were obtained with a MicroScribe-3DX digitizer (Immersion Corp, Salt Lake City, Utah) with HyperSpace Modeler software (Mira Imaging, Salt Lake City). The spatial resolution or accuracy of the system was 0.2 mm. In an effort to normalize the orientation across larynges, the origin for each larynx was defined as the most superior and anterior aspect of the cricoid ring in the midsagittal plane. After origin definition, the coordinates of the most posterior point on the cricoid prominence (between the right and left

PCA muscles) were acquired. This point was used as a reference to the origin to establish the y-axis by a translation in the negative y direction with respect to the x direction; changes in the z direction were ignored. The z-axis was established by acquiring a number of points along the cricoid prominence. The x-axis was then empirically established by its orthogonal relationships with the y- and z-axes.

By means of blunt dissection instruments, an individual muscle bundle was carefully isolated and partially separated from the rest of the muscle. Next, its points of origin and insertion were visually identified (Fig 2). In all cases, the geometric center of the point of muscle bundle attachment was used as an estimate of the insertion or origin for that bundle. The coordinates of origin and insertion of each bundle were digitized before the bundle was removed with tissue forceps and iris scissors. The mass of each muscle bundle was measured with a Mettler AE100 laboratory balance with a measurement reliability of 0.1 mg (Mettler Instruments, Hightstown, NJ). Throughout the dissection, saline solution was periodically applied to the larynx to keep the tissues from drying.

The muscles of interest were organized into the following groups: left and right PCAs (further separated into oblique and vertical portions); left and right LCAs; and left and right IAs (further separated into superior and inferior portions).

Geometric Descriptions of Muscles. For each muscle bundle, 6 points were recorded (3 for origin, 3 for insertion). The mean x, y, and z coordinates for each of the 3 samples were calculated to yield an average origin or insertion for each muscle bundle. The length l of each muscle bundle was then calculated from the Pythagorean theorem:

$$(1) \quad l = \sqrt{(x_2 - x_1)^2 + (y_2 - y_1)^2 + (z_2 - z_1)^2}$$

where x_1 , y_1 , and z_1 are the coordinates of the origin and x_2 , y_2 , and z_2 are those of the insertion. An orientation vector \mathbf{r} was defined for each muscle bundle as

$$(2) \quad \mathbf{r} = r_x \mathbf{i} + r_y \mathbf{j} + r_z \mathbf{k}$$

where \mathbf{i} , \mathbf{j} , and \mathbf{k} are unit vectors along the orthogonal axes, and that

$$(3) \quad r_x = x_2 - x_1$$

$$(4) \quad r_y = y_2 - y_1$$

$$(5) \quad r_z = z_2 - z_1$$

As the mass m of each bundle was measured and the length was calculated, the cross-sectional area A was determined by

$$(6) \quad A = \frac{m}{\rho l}$$

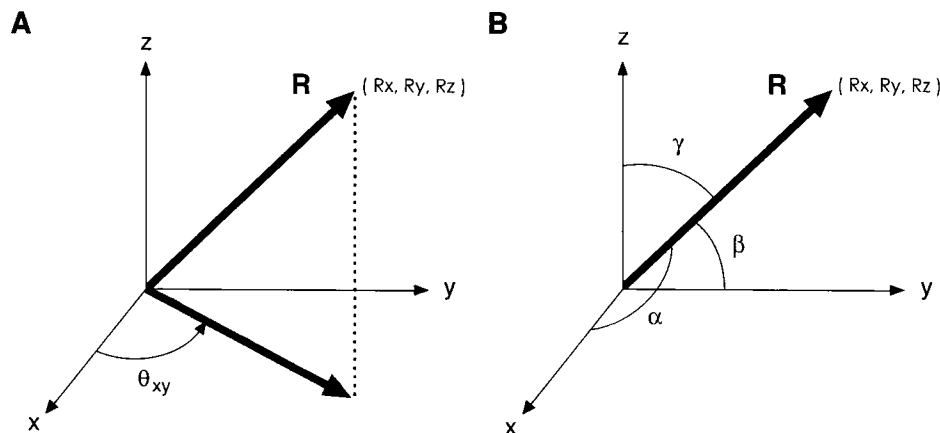


Fig 3. Three-dimensional illustration of A) 2-dimensional projection angle θ_{xy} of vector \mathbf{R} , and B) angles α , β , and γ of vector \mathbf{R} .

where ρ is the density of canine laryngeal muscle obtained previously (0.001043 g/mm^2).²⁰ The assumption here was that the muscle bundle has a uniform cross-sectional area along its entire course.

Resultant Vectors for Muscle Bundle Groups. The relative contribution of each muscle bundle to the total action of a muscle was estimated from cross-sectional area data. The orientation vector \mathbf{r} for each bundle was multiplied by that bundle's cross-sectional area A . This product was defined as the scaled force vector $\mathbf{r}A$. The assumption here was that all muscle fibers have equal contractile force per unit cross-sectional area. The scaled force vectors were summed and divided by the total cross-sectional area for that grouping of muscle bundles to yield an average resultant force vector \mathbf{R} ,

$$(7) \quad \mathbf{R} \equiv \mathbf{R}_x \mathbf{i} + \mathbf{R}_y \mathbf{j} + \mathbf{R}_z \mathbf{k} = \frac{\sum_{i=1}^n r_i A_i}{\sum_{i=1}^n A_i}$$

A resultant force vector was calculated for each of the following muscle bundle groups, or *muscle portions*: 1) left PCA, oblique portion (L PCA o); 2) left PCA, vertical portion (L PCA v); 3) right PCA, oblique portion (R PCA o); 4) right PCA, vertical portion (R PCA v); 5) left LCA (L LCA); 6) right LCA (R LCA); 7) left IA, inferior portion (L IA inf); 8) left IA, superior portion (L IA sup); 9) right IA, inferior portion (R IA inf); and 10) right IA, superior portion (R IA sup).

Data on the superior portion of the IA muscle are not reported, because its anatomy was found to be grossly different from that of humans. Our observations showed that it did not connect the 2 arytenoid cartilages together. Rather, both its origin and insertion appeared to originate from the same side in the canine larynx.

Planar Projection Angle Calculations. For 2-dimensional (2-D) planar analysis, the resultant force vector \mathbf{R} for each muscle portion was used to calculate the projection angle in each of the 3 orthogonal planes. The projection angle in the xy plane was calculated from the formula (Fig 3A)

$$(8) \quad \theta_{xy} = \tan^{-1} \frac{\mathbf{R}_y}{\mathbf{R}_x}$$

The positive x direction was medial-to-lateral on the right side, and the positive y direction was posterior-to-anterior. Angles were reported in standard fashion, with positive rotation defined as counter-clockwise from the x -axis toward the y -axis.

Projection angles in the yz and xz planes were similarly calculated for each muscle portion:

$$(9) \quad \theta_{yz} = \tan^{-1} \frac{\mathbf{R}_z}{\mathbf{R}_y}$$

$$(10) \quad \theta_{zx} = \tan^{-1} \frac{\mathbf{R}_x}{\mathbf{R}_z}$$

Thus, the xy plane was horizontal, the yz plane sagittal, and the xz plane coronal.

Direction Cosines. For the purpose of 3-D modeling, the direction cosines were also calculated. The direction cosines were defined as the cosine of the angle between a given resultant force vector \mathbf{R} and each of the 3 axes (Fig 3B),

$$(11) \quad \cos \alpha = \frac{\mathbf{R}_x}{\|\mathbf{R}\|} \quad \cos \beta = \frac{\mathbf{R}_y}{\|\mathbf{R}\|} \quad \cos \gamma = \frac{\mathbf{R}_z}{\|\mathbf{R}\|}$$

where $\|\mathbf{R}\|$ is the magnitude or length of the resultant force vector.

RESULTS AND DISCUSSION

Measurement Reliability. During the data acquisition process, there were 2 major sources of experimental and measurement errors. First, muscles and other soft tissues of the larynx sometimes showed

TABLE 2. MAGNITUDE OF MEASUREMENT ERRORS BY MUSCLE PORTION

	Length (mm)	Cross-sectional Area (mm ²)	θ_{xy} (°)	θ_{yz} (°)	θ_{zx} (°)
L PCA o	0.772 (5.20%)	0.207 (0.81%)	2.97 (1.65%)	2.42 (1.35%)	4.50 (2.78%)
L PCA v	1.277 (8.81%)	0.525 (4.99%)	6.03 (3.35%)	4.34 (2.41%)	3.90 (2.16%)
L PCA (total)	0.916 (6.22%)	0.298 (0.83%)	3.79 (2.10%)	2.94 (1.63%)	4.70 (2.61%)
R PCA o	0.755 (4.99%)	0.238 (1.07%)	2.41 (1.34%)	2.77 (1.54%)	4.86 (2.70%)
R PCA v	0.767 (5.05%)	0.271 (2.55%)	3.60 (2.00%)	2.29 (1.27%)	3.66 (2.03%)
R PCA (total)	0.759 (5.01%)	0.249 (0.76%)	2.80 (1.56%)	2.61 (1.45%)	4.46 (2.48%)
L LCA	0.791 (5.47%)	0.355 (1.65%)	2.18 (1.21%)	4.56 (2.53%)	14.18 (7.88%)
R LCA	0.850 (5.91%)	0.350 (1.68%)	3.15 (1.75%)	5.66 (3.15%)	9.42 (5.23%)
L IA inf	0.718 (8.02%)	0.746 (6.60%)	4.23 (2.35%)	3.81 (2.12%)	7.44 (4.13%)
R IA inf	0.714 (7.42%)	0.919 (7.06%)	4.82 (2.68%)	5.10 (2.83%)	8.49 (4.72%)
Mean error	0.792 (6.21%)	0.486 (2.80%)	3.49 (1.94%)	4.11 (2.28%)	8.11 (4.51%)
SD	0.168 (1.41%)	0.240 (2.47%)	1.18 (0.65%)	1.21 (0.67%)	3.32 (1.85%)

See text for abbreviations.

slight movement and deformation under the pressure of the digitizer probe. Second, external forces applied on the larynx during muscle bundle dissection sometimes also caused slight tissue movement and deformation. Because of these errors, there was some variability in the measured coordinates across different sampled points of the same muscle bundle insertion or origin.

Experimental error or variability of the data was quantified for dog 7, which was chosen because there were a large number of muscle bundles in each of its different muscle portions. Error in length measurement was estimated by first finding the maximum length possible based on the 3 origin data points and the 3 insertion data points for each muscle bundle. The maximum lengths were then averaged across bundles for each muscle portion. Table 2 shows the deviations between the maximum lengths and the average lengths for the 8 different muscle portions, and their percentage errors. As shown in Table 2, the mean error for all muscles was 6.2%.

The maximum possible cross-sectional area for

each bundle of dog 7 was calculated from equation 6 on the basis of the measured mass, the balance reliability (0.1 mg), and the average length data. The minimum possible cross-sectional area was calculated similarly, but it was based on the maximum calculated length for each bundle. The difference between the maximum and the minimum for each bundle was obtained, and an average was calculated for each muscle portion. Table 2 shows that the error ranged from about 1% to 7%. The maximum and minimum orientation angles (2-D projection angles) were calculated from the 3 origin points and the 3 insertion points for each bundle to estimate the error in vector calculations. The difference between these angles was obtained for each bundle, and an average error was computed for each muscle portion. Table 2 shows that the percentage error values, reported with respect to 180°, ranged from about 1% to 8%, with most of them smaller than 3%.

Muscle Mass, Length, Cross-Sectional Area, and Orientation. Table 3 shows the mass of each muscle portion for all subjects and their averages. It can be

TABLE 3. MASS OF CANINE LARYNGEAL ABDUCTOR AND ADDUCTOR MUSCLES

	Dog 1	Dog 2	Dog 3	Dog 4	Dog 5	Dog 6	Dog 7	Dog 8	Mean	SD
L PCA o	0.429	0.580	0.480	0.580	0.210	0.359	0.300	0.305	0.405	0.136
L PCA v	0.161	0.168	0.206	0.137	0.148	0.136	0.169	0.121	0.155	0.027
L PCA (total)	0.590	0.748	0.686	0.716	0.358	0.495	0.469	0.449	0.564	0.142
R PCA o	0.337	0.511	0.353	0.529	0.213	0.301	0.273	0.266	0.348	0.115
R PCA v	0.171	0.143	0.263	0.135	0.118	0.201	0.191	0.181	0.175	0.046
R PCA (total)	0.507	0.655	0.616	0.664	0.331	0.502	0.464	0.447	0.523	0.115
L LCA	0.273	0.351	0.402	0.466	0.184	0.346	0.268	0.269	0.320	0.089
R LCA	0.269	0.304	0.357	0.448	0.182	0.358	0.276	0.270	0.308	0.080
L IA inf	0.123	0.068	0.139	0.130	0.082	0.128	0.106	0.112	0.111	0.025
R IA inf	0.154	0.095	0.152	0.182	0.073	0.143	0.112	0.139	0.131	0.036
Total	1.916	2.221	2.351	2.607	1.210	1.972	1.695	1.686	1.957	0.439

Data are mass in grams.

TABLE 4. LENGTH OF CANINE LARYNGEAL ABDUCTOR AND ADDUCTOR MUSCLES

	<i>Dog 1</i>	<i>Dog 2</i>	<i>Dog 3</i>	<i>Dog 4</i>	<i>Dog 5</i>	<i>Dog 6</i>	<i>Dog 7</i>	<i>Dog 8</i>	<i>Mean</i>	<i>SD</i>
L PCA o	14.527	14.199	16.142	15.911	14.161	15.261	13.096	15.081	14.797	1.005
L PCA v	11.899	15.082	15.634	16.029	14.885	14.568	13.310	14.540	14.493	1.325
L PCA (total)	13.943	14.396	16.029	15.933	14.342	15.113	13.149	14.965	14.734	0.979
R PCA o	14.287	14.486	15.378	16.763	14.827	15.322	13.441	14.948	14.932	0.967
R PCA v	14.509	15.373	17.008	18.892	15.732	16.600	14.940	13.852	15.863	1.604
R PCA (total)	14.342	14.683	15.786	17.150	15.128	15.748	13.903	14.583	15.165	1.036
L LCA	13.259	14.993	14.768	14.918	13.913	15.394	14.431	13.976	14.457	0.701
R LCA	14.407	15.006	13.954	16.152	12.803	13.982	15.442	15.276	14.394	1.210
L IA inf	9.412	7.834	9.210	9.744	8.897	8.887	8.945	8.920	8.951	0.527
R IA inf	10.054	8.728	14.280	10.489	8.048	8.622	7.761	9.807	9.626	1.969

Data are in millimeters.

seen that the PCA muscle was always the most massive, whereas the IA muscle had the smallest mass, and the LCA muscle was in between. The oblique portion of the PCA muscle was consistently more massive than the vertical portion, in many cases by 2 to 3 times. The data also showed that muscles of the right and the left sides were basically symmetric to each other in terms of mass. These results were consistent with previous classic anatomic descriptions of the laryngeal abductor and adductor muscles.

Table 4 shows the lengths of the muscle portions, which were averages of individual muscle bundle lengths. Note that the lengths of the PCA muscle were not simple averages of those of the oblique and vertical portions, because there was always a larger number of muscle bundles in the oblique portion, as evidenced by its larger mass (Table 3). Nonetheless, the data showed that their lengths were quite similar to one another (mean differences <1 mm). The lengths of the LCA muscle were also close to those of the PCA muscle, whereas the IA muscle was about 30% to 50% shorter.

The cross-sectional area for each muscle bundle was estimated from the measured mass and the calculated length. The average cross-sectional area for

each muscle portion was calculated, and the results are shown in Table 5. Similar to the mass data, the PCA muscle was consistently the largest in cross-sectional area, whereas the LCA muscle was often about 40% smaller and the IA muscle was about 60% smaller. Also, the oblique portion of the PCA muscle was again about 2 to 3 times larger than the vertical portion.

Table 6 shows the average projection angles and direction cosines of the 8 muscle portions. The angles of orientation were averaged across all subjects. They were oriented such that the muscular process of the arytenoid cartilage was the geometric origin, and a positive angle was defined as rotating in a counterclockwise direction from x to y, y to z, or z to x.

Figure 4 illustrates the angles of the 2 portions of the PCA muscle on the xy, yz, and xz planes. The orientation angles of the arrows represent the lines of action of the muscle portions, whereas the lengths of the arrows are indications of their relative force magnitudes as they were scaled according to the muscle cross-sectional areas. Hence, the arrows represent projections of the resultant force vectors of the 2 PCA portions onto the 3 orthogonal planes. Not surprisingly, the oblique portion was always at a more

TABLE 5. CROSS-SECTIONAL AREA OF CANINE LARYNGEAL ABDUCTOR AND ADDUCTOR MUSCLES

	<i>Dog 1</i>	<i>Dog 2</i>	<i>Dog 3</i>	<i>Dog 4</i>	<i>Dog 5</i>	<i>Dog 6</i>	<i>Dog 7</i>	<i>Dog 8</i>	<i>Mean</i>	<i>SD</i>
L PCA o	27.20	38.10	27.95	33.46	14.03	22.13	21.44	19.04	25.42	7.86
L PCA v	13.02	10.42	12.96	8.12	9.54	8.89	12.03	9.21	10.52	1.91
L PCA (total)	40.22	48.52	40.91	41.58	23.57	31.02	33.47	28.25	35.94	8.24
R PCA o	22.84	33.32	21.73	29.89	14.29	18.99	19.47	17.34	22.23	6.41
R PCA v	11.26	8.92	14.82	6.87	7.16	11.47	12.18	12.46	10.64	2.77
R PCA (total)	34.10	42.25	36.55	36.76	21.44	30.46	31.65	29.80	32.88	6.16
L LCA	19.48	23.03	25.83	31.78	13.11	22.16	17.79	19.37	21.57	5.61
R LCA	17.82	19.60	23.91	26.63	14.05	25.12	17.55	17.61	20.80	4.41
L IA inf	12.81	8.34	14.44	12.83	8.94	13.73	11.34	12.01	11.30	2.54
R IA inf	14.71	10.47	14.41	16.55	8.84	15.77	13.88	13.73	13.02	2.90
Total	140.14	154.20	159.05	170.13	95.96	145.26	133.68	129.73	141.02	22.60

Data are in square millimeters as computed from muscle mass, length, and density (see equation 6 in text).

TABLE 6. MEAN PROJECTION ANGLES AND DIRECTION COSINES OF CANINE LARYNGEAL ABDUCTOR AND ADDUCTOR MUSCLES

	2-D Projection Angles (°)			3-D Direction Cosines		
	θ_{xy}	θ_{yz}	θ_{zx}	$\cos \alpha$	$\cos \beta$	$\cos \gamma$
L PCA o	-22.3	-115.5	130.7	0.739	-0.293	-0.607
L PCA v	-17.0	-97.2	157.6	0.372	-0.119	-0.920
L PCA (total)	-21.1	-108.6	139.0	0.647	-0.247	-0.721
R PCA o	-158.6	-117.6	-126.9	-0.759	-0.298	-0.579
R PCA v	-169.8	-94.3	-157.4	-0.413	-0.063	-0.909
R PCA (total)	-161.2	-107.4	-137.3	-0.666	-0.228	-0.710
L LCA	75.0	-25.6	150.9	0.238	0.869	-0.433
R LCA	99.7	-23.6	-158.6	-0.158	0.902	-0.403
L IA inf	-43.0	157.5	68.9	0.701	-0.660	0.269
R IA inf	-137.7	152.1	-64.3	-0.692	-0.627	0.358

oblique orientation than the vertical portion. It was also always stronger, especially its component on the xy plane.

Figure 5 summarizes the resultant force vectors of all 3 abductor and adductor muscles, namely, the LCA, PCA (the resultant of the 2 portions), and IA (the inferior portion). Again, the orientation angles represent their lines of action, whereas the lengths are estimations of the relative magnitudes of their forces projected onto the 3 planes. In terms of the orientation angles, the data were qualitatively consistent with classic descriptions of the muscles. The lines of action as shown in Fig 5 suggested that the LCA tends to pull the muscular process of the arytenoid cartilage anteriorly, inferiorly, and medially, thereby moving the vocal process medially and adducting the vocal fold. The PCA muscle, on the other hand, tends to move the muscular process posteriorly, inferiorly, and medially, abducting the vocal fold. Interestingly, the IA muscle seems to be somewhat of an antagonist of the LCA muscle on the basis of their orientation angles on the xy and yz planes. Nonetheless, its superior-medial direction of action as shown on the xz plane suggested that it might move the arytenoid

toward the midline, thereby adducting the vocal fold. These data on the average lines of action of the abductor and adductor muscles may be useful clinically for certain phonosurgical procedures. For example, data on the orientation angles of the LCA muscle may serve as quantitative guidelines for clinicians to establish a more physiological direction of the sutures used in arytenoid adduction.

In terms of the relative force magnitudes, the data suggested that the PCA muscle was always stronger than the LCA and IA muscles, especially on the xz plane, where it was 3 to 4 times stronger. The LCA muscle was slightly weaker than the PCA muscle on the xy and yz planes, but the difference was much larger on the xz plane. The IA muscle was always the weakest, especially on the yz plane, where it was 2 to 3 times weaker than the other two. These findings were consistent with the cross-sectional area data, as the muscle's resultant force vectors were computed partly on the basis of their cross-sectional areas. The assumption was that the maximum active stress was similar for the 3 different muscles, such that the relative magnitude of force generated by a muscle is proportional to its cross-sectional area.

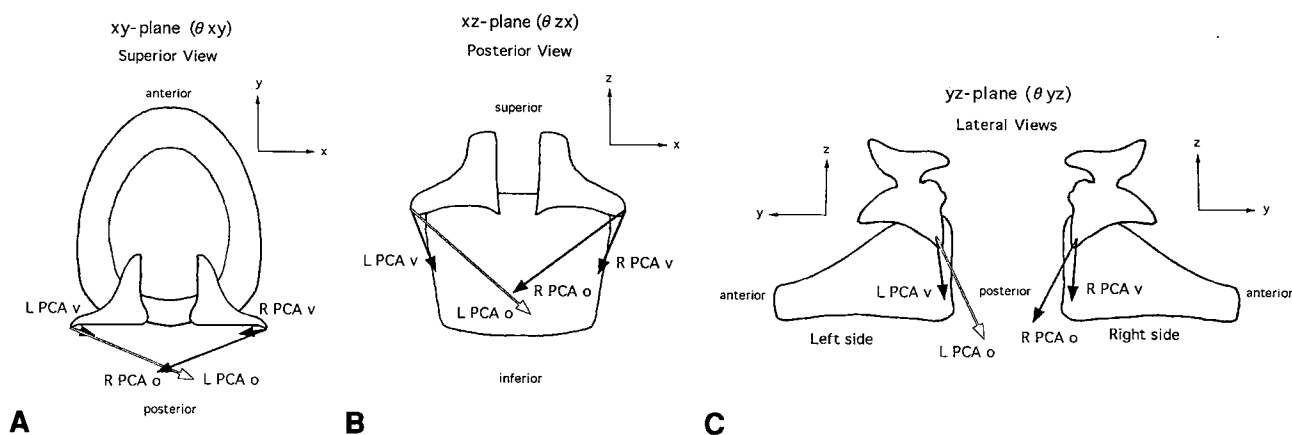


Fig 4. Resultant force vectors of oblique and vertical portions of PCA muscle. A) Superior view; vectors projected onto xy plane. B) Posterior view; vectors projected onto xz plane. C) Lateral views; vectors projected onto yz plane.

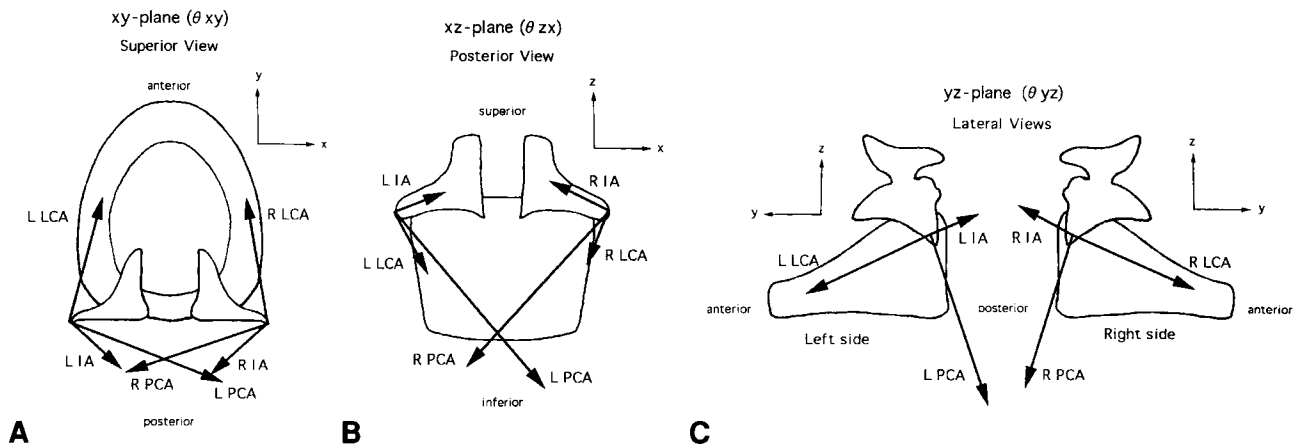


Fig 5. Resultant force vectors of PCA, LCA, and IA muscles. A) Superior view; vectors projected onto xy plane. B) Posterior view; vectors projected onto xz plane. C) Lateral views; vectors projected onto yz plane.

Limitations and Suggestions for Further Studies.

One limitation of the present study was that the calculations of muscle lengths and orientation angles were made by assuming that the muscle bundles form a straight line between the origin and insertion points. However, this was not always the case, especially for the PCA, in which muscle fibers often were seen to course around the curved laryngeal cartilage surfaces. Also, the fiber bundles on a muscle's surface were often more curved than the internal bundles. Such errors likely led to underestimations of length, overestimations of cross-sectional area, and discrepancies in estimations of the effective line of action in some of the muscles. In future experiments, increasing the number of sampling points for each bundle might help to reduce such errors. For example, by taking an extra data point at the midpoint of each muscle bundle, one can establish more accurate estimations of the muscle bundle length and its effective orientation angle on the basis of the best-fit curve for the 3 data points (origin, insertion, and midpoint).

During data collection, the cricoid and the arytenoid cartilages were securely fixed in the cadaveric position to minimize specimen movement and to ensure accurate measurements of the 3-D coordinates. However, slight movements of the cricoid and the arytenoid cartilages were still sometimes observed during muscle bundle resection and data acquisition. Such movements likely introduced random errors into the 3-D coordinate data sampled by the digitizer. In future experiments, extra pins or other devices should be used to more securely fix the cartilages so as to eliminate these errors.

Anatomic differences between the canine and human larynges must be acknowledged when canine data are used for modeling of the human larynx. The canine larynx is similar to the human larynx in terms of size, morphological features, and basic vocal fold anatomy, but there are also some significant differ-

ences. The human IA muscle consists of a transverse portion and an oblique portion, both of which clearly and consistently cross the midline. For the canine IA muscle, however, our observations showed that it can be divided into a superior portion and an inferior portion. The inferior portion was distinctly separated into left and right halves joined by a sheet of tendon-like connective tissue at the midline, whereas the superior portion stayed on the same arytenoid cartilage and extended anteriorly to insert into the structures above the arytenoid cartilage (the cuneiform and corniculate processes). Further, the arytenoid cartilages of dogs are proportionately larger than those of humans.

Considering such anatomic differences between the canine larynx and the human larynx, the 3-D characterization of the canine laryngeal muscles may only represent a rough approximation of the human muscles. However, the two species exhibit sufficient similarities in basic laryngeal anatomy that the canine model remains a valuable approximation of the human larynx.

CONCLUSIONS

The PCA, LCA, and IA muscles are important in the control of vocal fold abduction and adduction. These muscles function in a well-coordinated manner during phonation, respiration, and airway protection to allow for various adjustments of the anatomic orientations of the vocal folds. This study quantified the mass, length, relative cross-sectional area, and angle of orientation in 3-D space of these abductor and adductor muscles in 8 canine larynges. This 3-D anatomic characterization allowed for the calculations of average lines of action and moment arms for the muscles, providing important data for biomechanical modeling of vocal fold posturing. These data may also be useful in devising clinical guidelines for certain phonosurgical procedures such as arytenoid adduction.

REFERENCES

1. Sanders I, Jacobs I, Wu B-L, Biller HF. The three bellies of the canine posterior cricoarytenoid muscle: implications for understanding laryngeal function. *Laryngoscope* 1993;103:171-7.
2. Sanders I, Rao F, Biller HF. Arytenoid motion evoked by regional electrical stimulation of the canine posterior cricoarytenoid muscle. *Laryngoscope* 1994;104:456-62.
3. Sanders I, Wu B-L, Mu L, Li Y, Biller HF. The innervation of the human larynx. *Arch Otolaryngol Head Neck Surg* 1993;119:934-9.
4. Sanders I, Wu B-L, Mu L, Biller HF. The innervation of the human posterior cricoarytenoid muscle: evidence for at least two neuromuscular compartments. *Laryngoscope* 1994;104:880-4.
5. Alipour-Haghighi F, Titze IR, Perlman AL. Tetanic contraction in vocal fold muscle. *J Speech Hear Res* 1989;32:226-31.
6. Alipour-Haghighi F, Perlman AL, Titze IR. Tetanic response of the cricothyroid muscle. *Ann Otol Rhinol Laryngol* 1991;100:626-31.
7. Alipour F, Titze I. Active and passive characteristics of the canine cricothyroid muscles. *J Voice* 1999;13:1-10.
8. Sonesson B. Die funktionelle Anatomie des Cricoarytenoid Gelenkes. *Z Anat Entwicklungsgesch* 1959;121:292-303.
9. Frable MA. Computation of motion at the cricoarytenoid joint. *Arch Otolaryngol* 1961;73:551-6.
10. von Leden H, Moore P. The mechanics of the cricoarytenoid joint. *Arch Otolaryngol* 1961;73:541-50.
11. Ardran GM, Kemp FH. The mechanism of the larynx: Part I. The movement of the arytenoid and cricoid cartilages. *Br J Radiol* 1966;39:641-54.
12. Sellars IE, Sellars S. Cricoarytenoid joint structure and function. *J Laryngol Otol* 1983;97:1027-34.
13. Neuman TR, Hengesteg A, Lepage RP, Kaufman KR, Woodson GE. Three-dimensional motion of the arytenoid adduction procedure in cadaver larynges. *Ann Otol Rhinol Laryngol* 1994;103:265-70.
14. Selbie WS, Zhang L, Levine WS, Ludlow CL. Using joint geometry to determine the motion of the cricoarytenoid joint. *J Acoust Soc Am* 1998;103:1115-27.
15. Williams PL, Warwick R, eds. *Gray's anatomy*. 36th ed. New York, NY: Churchill Livingstone, 1980.
16. Kahane J. The cricoarytenoid joint: perspectives gained since von Leden and Moore (1961). *J Voice* (in press).
17. Martensson A, Skoglund CR. Contraction properties of intrinsic laryngeal muscles. *Acta Physiol Scand* 1964;60:318-36.
18. Bryant NJ, Woodson GE, Kaufman K, et al. Human posterior cricoarytenoid muscle compartments, anatomy and mechanics. *Arch Otolaryngol Head Neck Surg* 1996;122:1331-6.
19. Sanders I, Mu L, Wu B-L, Biller HF. The intramuscular nerve supply of the human lateral cricoarytenoid muscle. *Acta Otolaryngol (Stockh)* 1993;113:679-82.
20. Perlman AL, Titze IR. Development of an in vitro technique for measuring the elastic properties of vocal fold tissue. *J Speech Hear Res* 1988;31:288-98.